Hypocretin/orexin and nociceptin/orphanin FQ coordinately regulate analgesia in a mouse model of stress-induced analgesia

doi: 10.1172/JC135115

Hypocretin/orexin and nociceptin/orphanin FQ coordinately regulate analgesia in a mouse model of stress-induced analgesia

Xinmin Xie,[1,2] Jonathan P. Wisor,[1] Junko Hara,[1] Tara L. Crowder,[1] Robin LeWinter,[1] Taline V. Khroyan,[3] Akihiro Yamanaka,[4] Sabrina Diano,[5] Tamas L. Horvath,[5,6] Takeshi Sakurai,[4] Lawrence Toll,[1] and Thomas S. Kilduff[1]

[1]Biosciences Division, SRI International, Menlo Park, California, USA. [2]AfaSci Inc., Burlingame, California, USA. [3]Center for Health Sciences, SRI International, Menlo Park, California, USA. [4]Institute of Basic Medical Sciences, University of Tsukuba, Tsukuba, Ibaraki, Japan. [5]Department of Obstetrics, Gynecology & Reproductive Sciences and Department of Neurobiology and [6]Section of Comparative Medicine, Yale University School of Medicine, New Haven, Connecticut, USA.

Stress-induced analgesia (SIA) is a key component of the defensive behavioral "fight-or-flight" response. Although the neural substrates of SIA are incompletely understood, previous studies have implicated the hypocretin/orexin (Hcrt) and nociceptin/orphanin FQ (N/OFQ) peptidergic systems in the regulation of SIA. Using immunohistochemistry in brain tissue from wild-type mice, we identified N/OFQ-containing fibers forming synaptic contacts with Hcrt neurons at both the light and electron microscopic levels. Patch clamp recordings in GFP-tagged mouse Hcrt neurons revealed that N/OFQ hyperpolarized, decreased input resistance, and blocked the firing of action potentials in Hcrt neurons. N/OFQ postsynaptic effects were consistent with opening of a G protein–regulated inwardly rectifying K^+ (GIRK) channel. N/OFQ also modulated presynaptic release of GABA and glutamate onto Hcrt neurons in mouse hypothalamic slices. *Orexin/ataxin-3* mice, in which the Hcrt neurons degenerate, did not exhibit SIA, although analgesia was induced by i.c.v. administration of Hcrt-1. N/OFQ blocked SIA in wild-type mice, while coadministration of Hcrt-1 overcame N/OFQ inhibition of SIA. These results establish what is, to our knowledge, a novel interaction between the N/OFQ and Hcrt systems in which the corticotropin-releasing factor and N/OFQ systems coordinately modulate the Hcrt neurons to regulate SIA.

Introduction

Stress-induced analgesia (SIA) is a key component of the defensive behavioral response to prepare for fight or flight. Although an extensive literature has established roles for the hypothalamopituitary axis and corticotropin-releasing factor (CRF), in particular, as a central mediator of stress, the neural substrates of SIA are poorly understood.

The hypocretins (Hcrt, also known as orexins) (1, 2), neuropeptides whose cell bodies are restricted to the perifornical and lateral areas of the tuberal hypothalamus (PLH) (3, 4), are primarily known for involvement in the control of sleep and wakefulness, energy metabolism, reward, and addiction (5–7). However, the Hcrt system has also been implicated in nociception, the stress response, and SIA. The Hcrt-1 peptide is analgesic (8–10), CRF excites Hcrt cells through the CRF receptor 1 (11), and SIA is reduced in Hcrt-null mutant mice (12).

Nociceptin (N/OFQ; also known as orphanin FQ) (13, 14) is a neuropeptide that has also been implicated in a number of physiological functions including locomotion, feeding behavior, anxiety, memory, pain, and stress responses, particularly SIA (15, 16). N/OFQ administered centrally can completely block severe SIA (16). In contrast to Hcrt, N/OFQ cell bodies are widely distributed throughout the CNS (17).

Exaggerated or prolonged SIA has long been considered to be detrimental to performance; therefore, SIA must be critically regulated (18, 19). Because N/OFQ blocks SIA, for which Hcrt is required, we hypothesized that interaction between these peptidergic systems might be a critical component of SIA regulation. In this study, we present evidence from anatomical, cellular electrophysiological, and behavioral studies that establishes direct interaction between the Hcrt and N/OFQ systems. We show that N/OFQ makes synaptic contacts with Hcrt cells, that the N/OFQ peptide inhibits the activity of Hcrt cells via pre- and postsynaptic mechanisms, that Hcrt neurons are essential in the generation of SIA, and that N/OFQ blocks SIA via inhibition of Hcrt activity. These results indicate that the Hcrt and N/OFQ systems interact to coordinately modulate SIA.

Results

Anatomical evidence for N/OFQ innervation of Hcrt neurons. To assess the potential for interaction between the N/OFQ and Hcrt systems, we first determined whether N/OFQ fibers were present in the vicinity of Hcrt-synthesizing cell bodies using double-label immunohistochemistry. N/OFQ-containing fibers and Hcrt somata were detected on 10-μm sections incubated in anti-N/OFQ and anti–orexin-B antisera. Using fluorescent light and confocal microscopy, we observed the presence of N/OFQ-immunoreac-

Nonstandard abbreviations used: CRF, corticotropin-releasing factor; EC_{50}, 50% effective concentration; EPSC, excitatory postsynaptic current; GIRK, G protein–regulated inwardly rectifying K^+; Hcrt, hypocretin/orexin; IPSC, inhibitory postsynaptic current; I-V, current-voltage; mEPSC, miniature EPSC; mIPSC, miniature IPSC; N/OFQ, nociceptin/orphanin FQ; PB, phosphate buffer; PLH, perifornical and lateral areas of the tuberal hypothalamus; sEPSC, spontaneous EPSC; SIA, stress-induced analgesia; sIPSC, spontaneous IPSC; TTX, tetrodotoxin; V_h, holding potential.

Conflict of interest: The authors have declared that no conflict of interest exists.

Citation for this article: *J. Clin. Invest.* **118**:2471–2481 (2008). doi:10.1172/JCI35115.

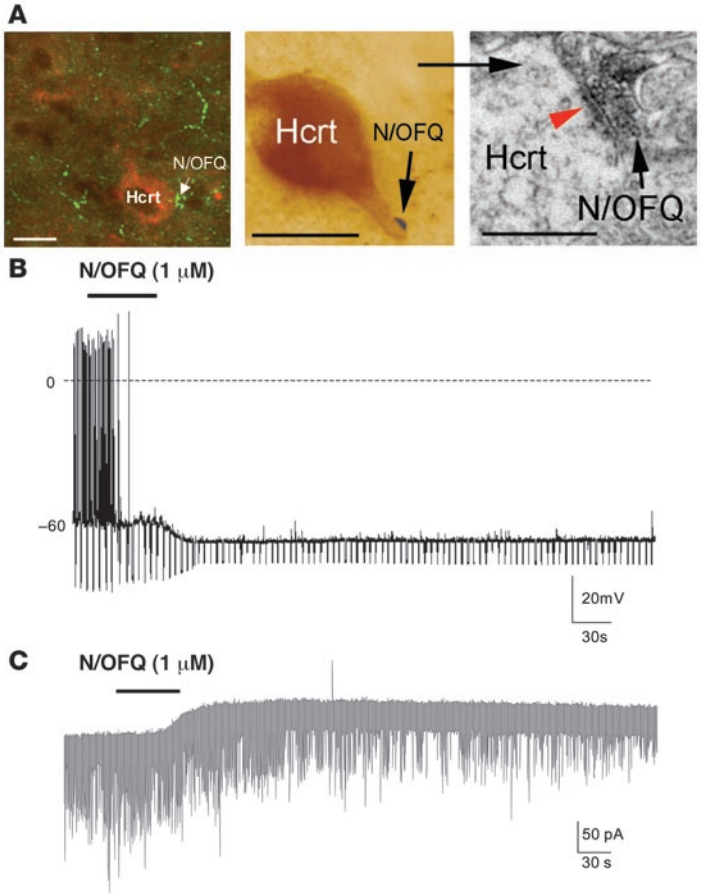

Figure 1
N/OFQ-containing fibers innervate Hcrt neurons, and N/OFQ inhibits Hcrt neuronal activity. (**A**) Left panel shows confocal image of N/OFQ-immunoreactive fibers in the vicinity of, and in putative contact with, Hcrt-immunoreactive neurons in the PLH of WT mice. N/OFQ (green) fibers are in close proximity to Hcrt-immunoreactive (red) cells. The arrow indicates the N/OFQ innervation of an Hcrt cell body. Middle panel shows light micrograph of a light brown immunolabeled Hcrt neuron contacted by a dark black bouton (arrow) representing immunolabeling for N/OFQ. Right panel shows electron micrograph taken from ultrathin sections of the same labeled terminal and dendrite shown in the light micrograph in the middle panel. Black arrow indicates the N/OFQ-immunolabeled axon terminal in synaptic contact (red arrowhead) with the dendrite of the Hcrt cell. Scale bars: 10 μm (left and middle panels); 1 μm (right panel). (**B**) Under current clamp, bath application of N/OFQ (1 μM) hyperpolarized Hcrt neurons, decreased input resistance, and blocked spontaneous firing of action potentials. The resting potential of this cell was –54 mV and was manually adjusted to –60 mV with DC current. Membrane resistance was monitored using hyperpolarizing current pulses (–0.3 nA, 800 ms) delivered every 5 seconds throughout the experiment. (**C**) Under voltage-clamp mode at a V_h of –60 mV, N/OFQ (1 μM) induced an outward current (–53 pA) in an Hcrt neuron. Notice that the frequency but not the amplitude of the miniature synaptic currents (inward currents) recorded in the presence of TTX (0.5 μM) was also reduced.

tive fibers in the vicinity of, and in putative contact with, Hcrt-immunoreactive neurons in the PLH of WT mice (Figure 1A). We then evaluated whether these 2 systems are synaptically connected through correlated light and EM analyses. As shown in Figure 1A, a light brown immunolabeled Hcrt neuron appears to be contacted by a dark black bouton immunolabeled for N/OFQ. Color photographs and images were taken of Hcrt-immunoreactive cells contacted by putative N/OFQ-immunoreactive axon terminals. Blocks were trimmed using the color picture of previously identified cells and boutons as a guide. Ribbons of serial ultrathin sections were collected on Formvar-coated single-slot grids and examined under the EM. Figure 1A presents an example of an N/OFQ-immunolabeled axon terminal evidently in synaptic contact with an Hcrt-immunolabeled dendrite.

Electrophysiological evidence for N/OFQ effects on Hcrt neurons. Functional modulation of Hcrt neurons by N/OFQ was evaluated using whole-cell patch clamp recordings of visually identified Hcrt neurons from transgenic mice in which EGFP was linked to the *hcrt/orexin* promoter (*orexin/EGFP* mice) (20, 21). (Although the terms are effectively synonymous, since the use of "hypocretin" [ref. 1] predates that of "orexin" [ref. 2] in the literature, we will refer to this neuropeptidergic system as "hypocretin," or "Hcrt." To avoid ambiguity, however, we will refer to the mouse models studied in this paper using the names by which they were originally described in the literature, viz., *orexin/EGFP* [refs. 21–23], *orexin/yellow cameleon 2.1* [ref. 24], and *orexin/ataxin-3* [ref. 25]). Brain slices (250 μm) containing the PLH were prepared, and *orexin/EGFP* (i.e., Hcrt) neurons were identified under fluorescence illumination; the same neuron was visualized using infrared differential interference contrast microscopy to guide electrode placement for patch clamp recording.

The electrophysiological characteristics of the Hcrt neurons recorded were consistent with those reported previously (20): V_m = –54 ± 0.9 mV, where V_m indicates membrane potential (n = 32). Bath application of N/OFQ (1 μM for 1 minute) caused a long-lasting hyperpolarization (8 ± 2.5 mV, n = 7), decreased input resistance (to 55% ± 8%), and complete blockade of the spontaneous firing of Hcrt neurons (Figure 1B). Membrane potential and cell excitability recovered approximately 20 minutes after washout of N/OFQ. To determine whether N/OFQ directly inhibited Hcrt neurons, N/OFQ was applied in the presence of tetrodotoxin (TTX) (0.3 μM) and recorded under voltage-clamp mode at a holding potential (V_h) of –60 mV. As shown in Figure 1C, N/OFQ (1 μM) consistently induced outward currents (42 ± 1 pA, n = 3), indicating a direct postsynaptic effect. N/OFQ-induced outward currents were associated with a decrease in frequency of miniature postsynaptic currents (2.7 ± 1.3 Hz in control vs. 1.4 ± 0.9 Hz in N/OFQ) but not amplitude (50 ± 9 pA in control vs. 55 ± 5 pA in N/OFQ), suggesting a presynaptic action as well (see below).

Under current-clamp mode, the postsynaptic responses (hyperpolarization and decreased input resistance) to N/OFQ were reversibly blocked by activation of the N/OFQ (NOP) receptor antagonist SR14148 (26) at 10 μM (Figure 2; n = 9), further confirming mediation by the NOP receptor. Since the N/OFQ-induced hyperpolarization apparently did not differ in the presence or absence of TTX, we pooled both data sets to construct a concentration-dependent

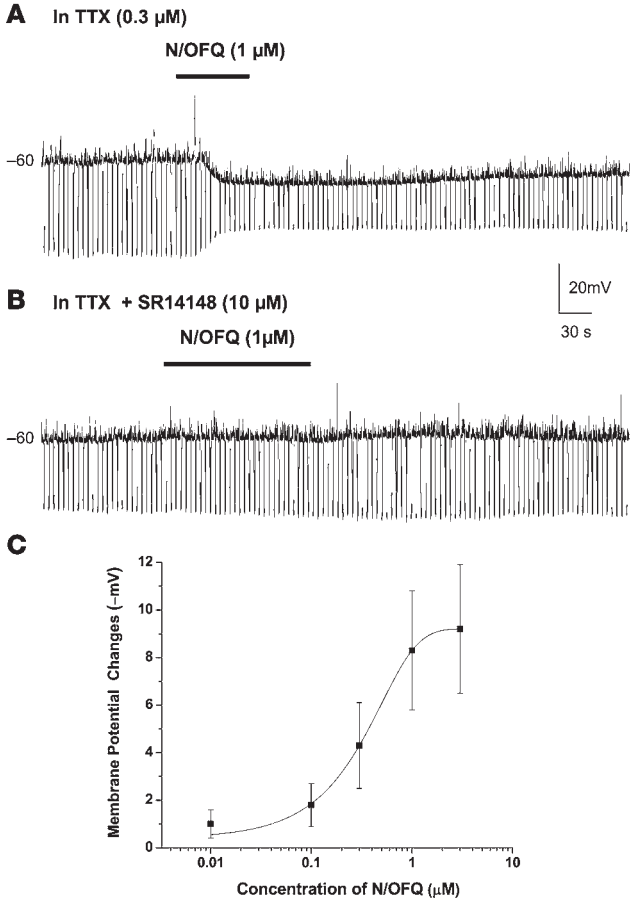

Figure 2
N/OFQ directly hyperpolarizes Hcrt neurons in a dose-depenedent manner. (**A**) N/OFQ (1 μM) caused hyperpolarization and a decrease in input resistance in the presence of TTX (0.3 μM), which was used to block synaptic activity and action potentials in an Hcrt-containing cell. (**B**) In the same neuron, the NOP receptor antagonist SR14148 (10 μM) blocks the N/OFQ-induced hyperpolarization and input resistance decrease. The blockade was reversible after 20-minute washout of the antagonist (data not shown). (**C**) Since the N/OFQ-induced hyperpolarization apparently did not differ in the presence or absence of TTX, both data sets were pooled to construct a concentration-dependent response curve using the pharmacologic dose-response model-fitting function (OriginPro 7.5; OriginLab). The half-maximal effect of N/OFQ-induced hyperpolarization (EC_{50}) was calculated at 0.329 μM with a Hill coefficient of 1.1. Error bars represent SEM.

response curve (Figure 2C). Using a dose-response model (OriginPro 7.5; OriginLab), we determined the half-maximal effect of N/OFQ-induced hyperpolarization (50% effective concentration [EC_{50}]) as approximately 0.3 μM with a Hill coefficient of 1.1, suggesting a single binding site.

N/OFQ affects membrane currents and intracellular calcium levels in Hcrt neurons. We evaluated the current-voltage (I-V) relationship of Hcrt neuronal responses in the presence and absence of N/OFQ (Figure 3, A and B). The I-V plot indicated a reversal potential of the N/OFQ-induced response at –108 ± 6 mV (n = 5; Figure 3C), close to the K^+ equilibrium potential (approximately –110 mV) under our experimental conditions, presumably mediated through activation of G protein–coupled inwardly rectifying K^+ (GIRK) channels (27). Together with the data in Figure 2, these results suggest the presence of functional NOP receptors on Hcrt cells in the hypothalamus.

Because N/OFQ has been shown to inhibit voltage-gated Ca^{2+} channels in other brain regions, we sought to determine its effect on intracellular Ca^{2+} levels in Hcrt neurons using 2 approaches. First, under conditions that block voltage-gated Na^+ and K^+ channels, depolarizing the membrane from a V_h of –60 mV to +20 mV evoked a high-voltage–activated Ca^{2+} current. N/OFQ (1 μM) inhibited the Ca^{2+} current to 88% ± 4.5% of control (P = 0.008, n = 7; Figure 3D). The residual current was completely blocked by Cd^{2+}, confirming that it was a Ca^{2+} current. Second, we used transgenic mice (*orexin/YC2.1*) in which Hcrt neurons specifically express the yellow cameleon calcium-sensing protein (24). Ca^{2+} imaging of Hcrt neurons from these mice revealed that N/OFQ inhibited intracellular Ca^{2+} concentration in 18 of 28 of the Hcrt neurons tested (Figure 3E); this effect was concentration dependent, with an EC_{50} of approximately 50 nM (Figure 3F).

N/OFQ inhibits Hcrt neurons by presynaptic and postsynaptic mechanisms. We next tested the effect of N/OFQ on spontaneous excitatory postsynaptic currents (sEPSCs) and spontaneous inhibitory postsynaptic currents (sIPSCs) under voltage-clamp mode. $GABA_A$ receptors were blocked with 50 μM bicuculline and 100 μM picrotoxin to pharmacologically isolate sEPSCs. Under voltage clamp with V_h = –60 mV, the mean frequency of sEPSCs was 6.0 ± 1.5 Hz (n = 4). We found that N/OFQ (1 μM) decreased the frequency of sEPSCs to 69% ± 5.3% of control values (n = 4; P < 0.01), with little effect on the amplitude of these events (Figure 4). Partial recovery was observed after washout of N/OFQ.

In a separate set of cells, we recorded the frequency and amplitude of sIPSCs in the presence of NMDA and α-amino-3-hydroxy-5-methyl-4-isoxazolepropionic acid (AMPA) receptor antagonists DL-2-amino-5-phosphonopentanoic acid (AP-5) (40 μM) and 6,7-dinitroquinoxaline-2,3-dione (DNQX) (40 μM), respectively, to block excitatory synaptic transmission (Figure 5). Under these conditions, the mean frequency of sIPSCs recorded from Hcrt neurons was 2.3 ± 0.5 Hz (n = 4). Bath application of 1 μM N/OFQ also significantly inhibited the frequency of sIPSCs to 48% ± 7.7% (n = 4; P < 0.05) but had no effect on the amplitude of these events. In some cells, the frequency of synaptic events recovered after prolonged washout of the peptide.

To determine whether N/OFQ acts directly at presynaptic terminals to decrease the probability of glutamate and GABA release, we examined the effects of NOP receptor activation on the frequency and amplitude of miniature EPSCs (mEPSCs) and IPSCs (mIPSCs). mEPSCs and mIPSCs were recorded in voltage clamp at a V_h of –60 mV. mEPSCs were pharmacologically isolated by adding bicuculline (20 μM), picrotoxin (100 μM), and TTX (0.5 μM) to the external solution. Under these conditions, the mean frequency of mEPSCs was 0.58 ± 0.08 Hz (n = 8). Bath application of N/OFQ (1 μM) significantly decreased the frequency of mEPSCs to 54% ± 7.1% of control (P = 0.002); the amplitude of these events was not significantly altered by NOP receptor activation (Figure 6A). mIPSCs were isolated by adding DNQX (40 μM), AP-5 (40 μM), and TTX (0.5 μM) to the external solution. Under these conditions, the mean frequency of mIPSCs was 0.36 ± 0.07 Hz (n = 8). Bath application of N/OFQ (1 μM) decreased the frequency of mIPSCs to 72% ± 22% of control (P = 0.02; Figure 6B), without a significant effect on

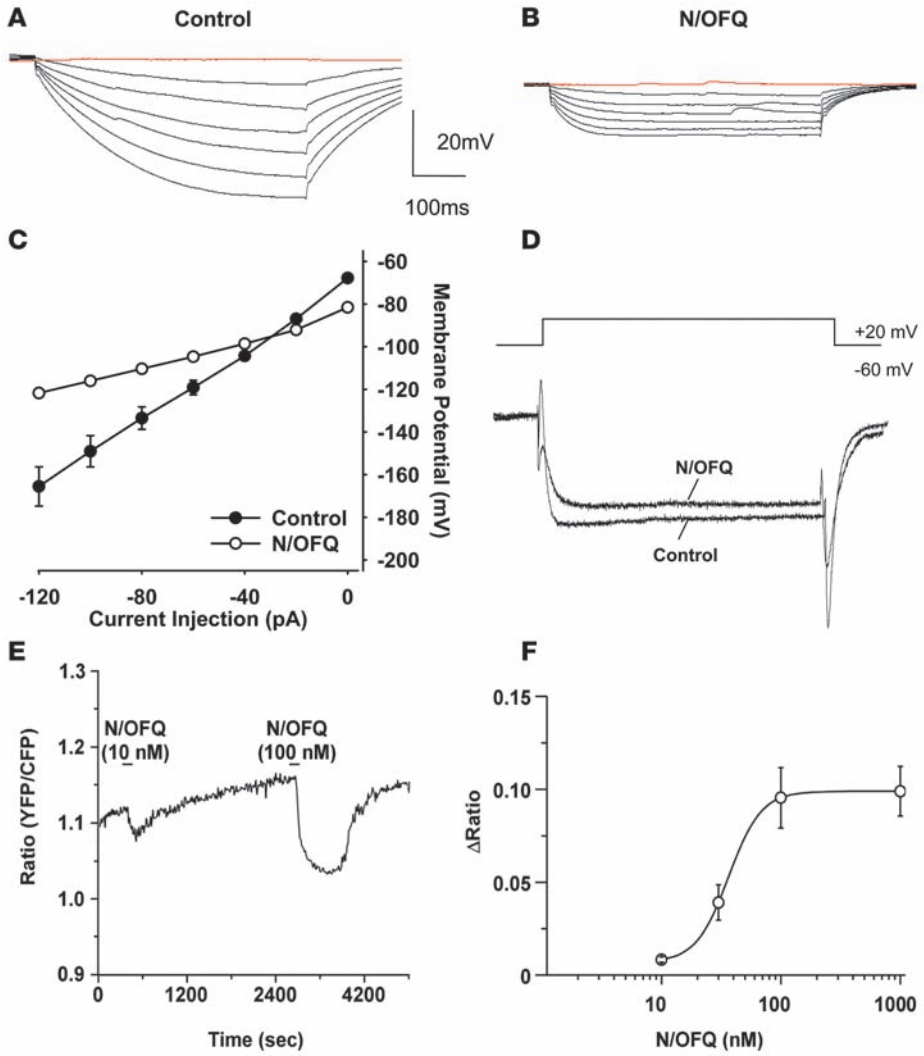

Figure 3
N/OFQ modulates membrane currents and depresses intracellular Ca^{2+} levels. (**A**–**C**) N/OFQ activates a K^+ conductance. The I-V relationship of neuronal responses in the presence (**B**) and absence (**A**) of N/OFQ (1 μM) indicates a reversal potential of –98 mV (**C**), which is close to the K^+ equilibrium potential (approximately –110 mV) under our experimental conditions. Before N/OFQ application, membrane potential was adjusted to a resting level of –60 mV by DC current injection. (**D**) N/OFQ inhibits Ca^{2+} currents. From a V_h of –60 mV, membrane voltage was stepped to +20 mV, which elicited an inward current. N/OFQ (1 μM) inhibited this current. Partial recovery was obtained after washout of N/OFQ, and the recovered current was completely blocked by Cd^{2+} (200 μM, data not shown). (**E**) N/OFQ depresses cytoplasmic Ca^{2+} in Hcrt neurons. Representative trace demonstrating the effect of N/OFQ on Ca^{2+} fluorescence in transgenic *orexin/YC2.1* mice in which Hcrt neurons express the calcium-sensing protein yellow cameleon 2.1. Ca^{2+} imaging from these mice revealed that N/OFQ inhibited approximately 65% of Hcrt neurons tested (18 of 28). (**F**) Concentration-dependent depression of cytoplasmic Ca^{2+} in Hcrt neurons induced by N/OFQ (mean ± SEM; n = 6–13 cells per concentration).

mIPSC amplitude. These results suggest that NOP activation can presynaptically decrease the release of both glutamate and GABA onto Hcrt neurons in the PLH.

A critical role for Hcrt neurons in SIA. To determine a functional role in vivo for a N/OFQ-Hcrt interaction, we investigated a behavior for which these 2 neuropeptides have been demonstrated to exhibit inverse actions: SIA. Previous studies had identified the Hcrt system as part of the CRF-mediated stress response (11) and showed that SIA is reduced in *prepro-hcrt* KO mice (12). To confirm the involvement of Hcrt in SIA, we used *orexin/ataxin-3* mice, a transgenic strain in which the Hcrt cells degenerate postnatally and are completely lost by adulthood (25). We first verified that our colony of *orexin/ataxin-3* mice showed greatly reduced levels of *prepro-hcrt* mRNA at the age of 10–13 weeks ($P < 0.01$; $t = 16.15$, degrees of freedom [*df*] = 9; Supplemental Figure 1A; supplemental material available online with this article; doi:10.1172/JCI35115DS1). To confirm the behavioral phenotype described previously in these mice (25), we measured overall activity and immobility using infrared video recordings. Episodes of "behavioral arrests" and complete immobility were apparent in some recordings; their occurrence and duration were determined by visual inspection of recordings by an experimenter blind to the genotypes. During the first 2 hours of the dark period, *orexin/ataxin-3* mice displayed 13 ± 2.9 (n = 6) immobile episodes compared with 1.8 ± 0.8 (n = 6) immobile episodes in WT mice from the same breeding colony ($P < 0.05$) and spent significantly more time in the immobile state than WT mice (Supplemental Figure 1B).

Having established a phenotype indicative of severe Hcrt neuron loss within our colony, we next assessed whether *orexin/ataxin-3* and WT mice differed in baseline thermal pain threshold. Using the conventional hot-plate and tail-flick tests, the thermal pain threshold did not differ between these 2 genotypes in either test (Supplemental Figure 1, C and D), consistent with previous observations in *prepro-hcrt* KO mice (12).

To investigate the necessity for an intact Hcrt system in SIA, we used restraint immobilization as the stressor to induce SIA in *orexin/ataxin-3* mice and WT littermates. Individual mice were immobilized within a plastic syringe (35 or 50 ml in proportion to body weight) for 30 minutes, and the hot-plate test (52°C) was performed within 1 minute after termination of the restraint. Restrained WT, but not ataxin, mice exhibited acute SIA (Figure 7A), as indicated by a significant increase in hind-paw withdrawal latency compared with control unrestrained mice kept in their home cage for 30 minutes prior to testing ($P < 0.01$; $F_{5,25} = 3.88$).

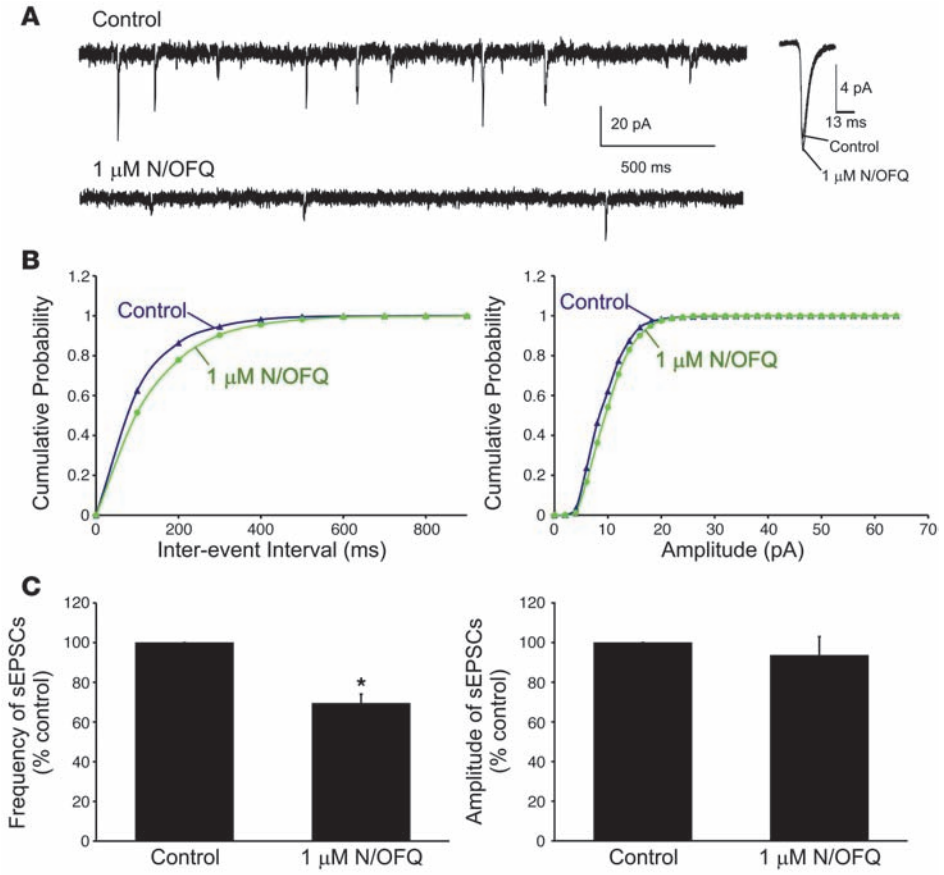

Figure 4
N/OFQ significantly decreases the frequency, but not the amplitude, of sEPSCs in Hcrt neurons. (**A**) Representative traces demonstrating the effect of N/OFQ on sEPSCs (left). Average sEPSCs from the same cell in the presence and absence of N/OFQ (1 μM, right). (**B**) Cumulative probability distributions of inter-event interval and amplitude for the cell shown in **A**. (**C**) Average effect of N/OFQ on sEPSC frequency and amplitude (n = 4). Cells were voltage clamped at –60 mV using a CsCl internal solution. Error bars represent SEM. *P < 0.05.

Since under our experimental conditions, SIA was evident in the hot-plate but not the tail-flick test (data not shown; P > 0.05), we focused on the hot-plate test in this study. The hot-plate pain test likely involves higher nociceptive transmission, whereas the tail-flick response to a focused thermal stimulus directed to the tail appears to be an involuntary spinally mediated reflex (28). Hind-paw withdrawal latency in the hot-plate test returned to baseline levels 30 minutes after the termination of stress, indicating cessation of SIA (Figure 7A). Hot-plate latency for the ataxin mice remained at basal levels, indicating the absence of SIA in this strain. Thus, in all subsequent SIA tests, we report the time point immediately after termination of restraint or the analogous time point for unrestrained control mice. As shown in Figure 7B, restraint caused a 50% ± 19% (n = 8) increase in hind-paw withdrawal latency in WT but not in *orexin/ataxin-3* mice. Two-way ANOVA with genotype (WT vs. ataxin) and treatment (restrained vs. unrestrained) as grouping variables revealed a significant genotype X treatment interaction (P < 0.02; $F_{1,26}$ = 7.421). Fisher's protected least significant difference test (PLSD) indicated that the latency was significantly greater in restrained WT mice than in WT mice not subjected to restraint (P < 0.05); no such effect was observed in *orexin/ataxin-3* mice (P > 0.4), indicating that the development of SIA is critically dependent on an intact Hcrt system.

We further evaluated whether an abrupt increase in Hcrt signaling by i.c.v. administration of exogenous Hcrt-1 was sufficient to produce an acute analgesic response in *orexin/ataxin-3* animals. *Orexin/ataxin*-3 mice were assigned to 1 of 4 groups (n = 13–14/group): i.c.v. vehicle/control; i.c.v. vehicle/restrained; i.c.v. Hcrt-1 (1.5 nmol/mouse)/control; and i.c.v. Hcrt-1 (1.5 nmol/mouse)/restrained. As indicated in Figure 7C, there was a significant antinociceptive effect of i.c.v. Hcrt-1 treatment (P < 0.05; $F_{1,50}$ = 4.348) with no effect of restraint in *orexin/ataxin*-3 mice. Consistent with noninjected restrained *orexin/ataxin*-3 mice (Figure 7B), SIA was absent in *orexin/ataxin*-3 mice following restraint. However, exogenous Hcrt-1 caused significant analgesia, apparently mimicking SIA.

N/OFQ-mediated inhibition of SIA is restored by Hcrt treatment. N/OFQ is known to inhibit SIA (16), although the neuronal pathways that mediate N/OFQ effects on SIA are still poorly understood. Since N/OFQ inhibits SIA and Hcrt appears to be necessary for SIA (Figure 7, B and C), we hypothesized that acute suppression of Hcrt signaling was the mechanism by which N/OFQ inhibited SIA and, therefore, i.c.v. coadministration of Hcrt should restore SIA in WT mice treated with N/OFQ. To test this hypothesis, we assessed the effects, separately and in combination, of i.c.v., Hcrt-1, and N/OFQ on SIA in WT mice. Figure 7D illustrates the results obtained when Hcrt-1 (1.5 nmol/mouse) or vehicle was injected i.c.v. in WT mice that had either been subjected to restraint or not. Two-way ANOVA with condition (restrained vs. unrestrained) and peptide treatment (Hcrt-1 vs. vehicle) as grouping variables revealed a significant effect of restraint (P < 0.03; $F_{1,28}$ = 5.903), indicating that SIA was robust after acute i.c.v. vehicle injection. Unlike in *orexin/ataxin-3* mice (Figure 7C), exogenous Hcrt-1 at 1.5 nmol/mouse did not produce a significant increase in hind-paw withdrawal latency in either restrained or unrestrained WT mice (Figure 7D), suggesting that restraint stress may induce maximal activation of the endogenous Hcrt system.

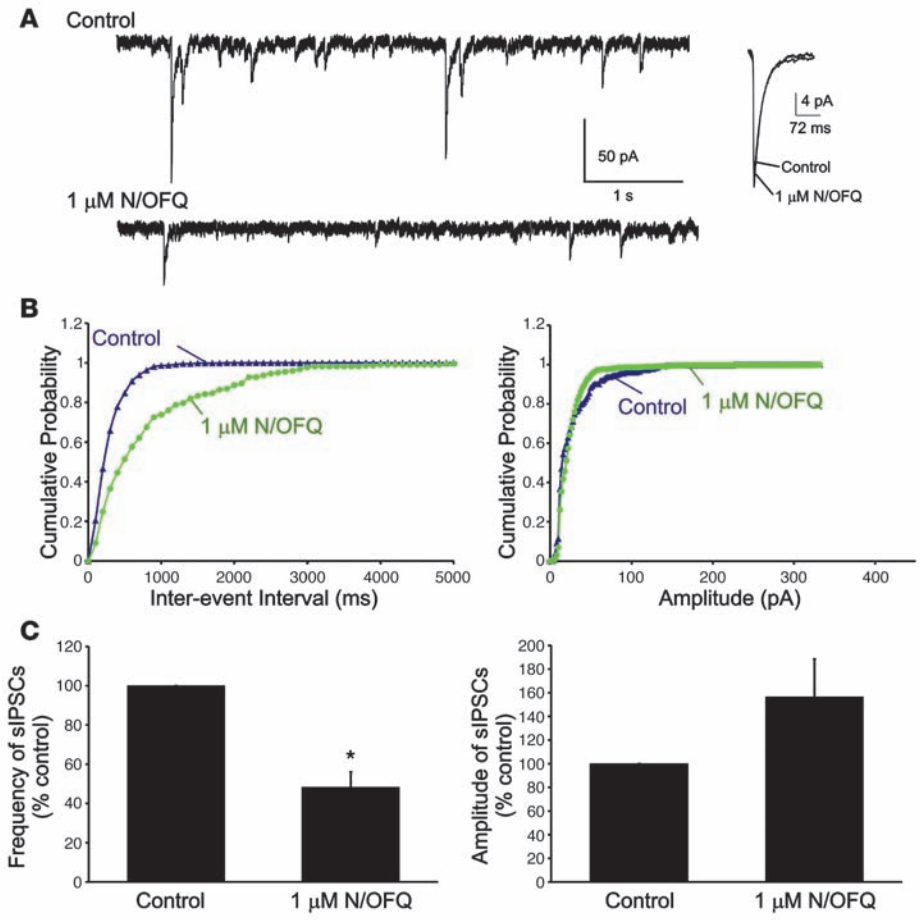

Figure 5
N/OFQ significantly decreases the frequency, but not the amplitude, of sIPSCs in Hcrt neurons. (**A**) Representative traces demonstrating the effect of N/OFQ on sIPSCs (left). Average sIPSCs from the same cell in the presence and absence of N/OFQ (1 μM, right). (**B**) Cumulative probability distributions for inter-event interval and amplitude for the cell shown in **A**. (**C**) Average effect of N/OFQ on sIPSC frequency and amplitude ($n = 4$). Cells were voltage clamped at –60 mV using a KCl internal solution. Error bars represent SEM. $^*P < 0.05$.

To directly test the hypothesis that Hcrt and N/OFQ interact in the regulation of SIA, we assessed the effects of i.c.v. Hcrt-1 and N/OFQ on SIA in WT mice. We initially evaluated 2 doses of N/OFQ in WT mice and found that N/OFQ at both 1 nmol/mouse and 3 nmol/mouse, administered i.c.v. immediately prior to restraint, produced complete blockade of SIA (data not shown). Thus, in subsequent tests, the lower dose of N/OFQ (1 nmol/mouse) was used and consistently produced blockade of SIA (Figure 7E). In unrestrained mice, N/OFQ (1 nmol/mouse) had no effect on hot-plate latency in the presence or absence of Hcrt-1. However, when Hcrt-1 (1.5 nmol/mouse) was coadministered with N/OFQ (1.0 nmol/mouse) to restrained WT mice, paw withdrawal latency was not significantly different than in mice administered vehicle prior to restraint (Figure 7E). Thus, Hcrt-1 treatment "rescued" the inhibition of SIA by N/OFQ.

Discussion

The results presented above demonstrate that N/OFQ fibers make synaptic contacts with Hcrt neurons (Figure 1) and that N/OFQ inhibits the activity of Hcrt neurons both directly by opening GIRK channels (Figures 1–3) and through indirect presynaptic mechanisms (Figures 4–6). At a systems level, we found that Hcrt neurons are essential for the production of SIA (Figure 7, A and B). Hcrt replacement can mimic SIA, which is otherwise absent in *orexin/ataxin-3* mice (Figure 7C), probably by activating the same downstream pathway as stress. Finally, N/OFQ inhibits SIA in WT mice, which can be recovered by coadministration of Hcrt (Figure 7E). Taken together, these results suggest that Hcrt neurons are a critical component for the production of SIA and that the well-established N/OFQ blockade of SIA is likely mediated through inhibition of Hcrt neuronal activity.

Although there are fewer than 5,000 Hcrt cells in the rodent (4) and about 70,000 cells in the human (29) brain, the widespread anatomical nature of Hcrt-containing fiber projections suggests that this system might serve multiple functions (4). Initially thought to be involved in food-intake regulation, the Hcrt system is now widely recognized as a central neurotransmitter system in the maintenance of wakefulness (5, 7). Defects in this system, either presynaptically or postsynaptically, result in the sleep disorder narcolepsy in both humans (29, 30) and animals (25, 31–33). Converging lines of evidence also indicate roles for the Hcrt system in energy metabolism (21, 25), cardiovascular control, reproductive and stress hormone secretion (34), reward and addiction (6, 35–37), and modulation of pain transmission by activating inhibitory pathways (12).

In contrast to the Hcrt system, N/OFQ mRNA and immunoreactive cell bodies are widely distributed throughout the CNS (17) as is the NOP receptor (38). Using both fluorescent light and confocal microscopy, N/OFQ-containing fibers were localized in the vicinity of Hcrt-synthesizing cell bodies using double-label immunohistochemistry (Figure 1A). Correlated light and EM analyses identified N/OFQ-immunolabeled boutons in contact with Hcrt-immunolabeled neurons and N/OFQ-immunolabeled axon terminals in synaptic contact with Hcrt-immunolabeled

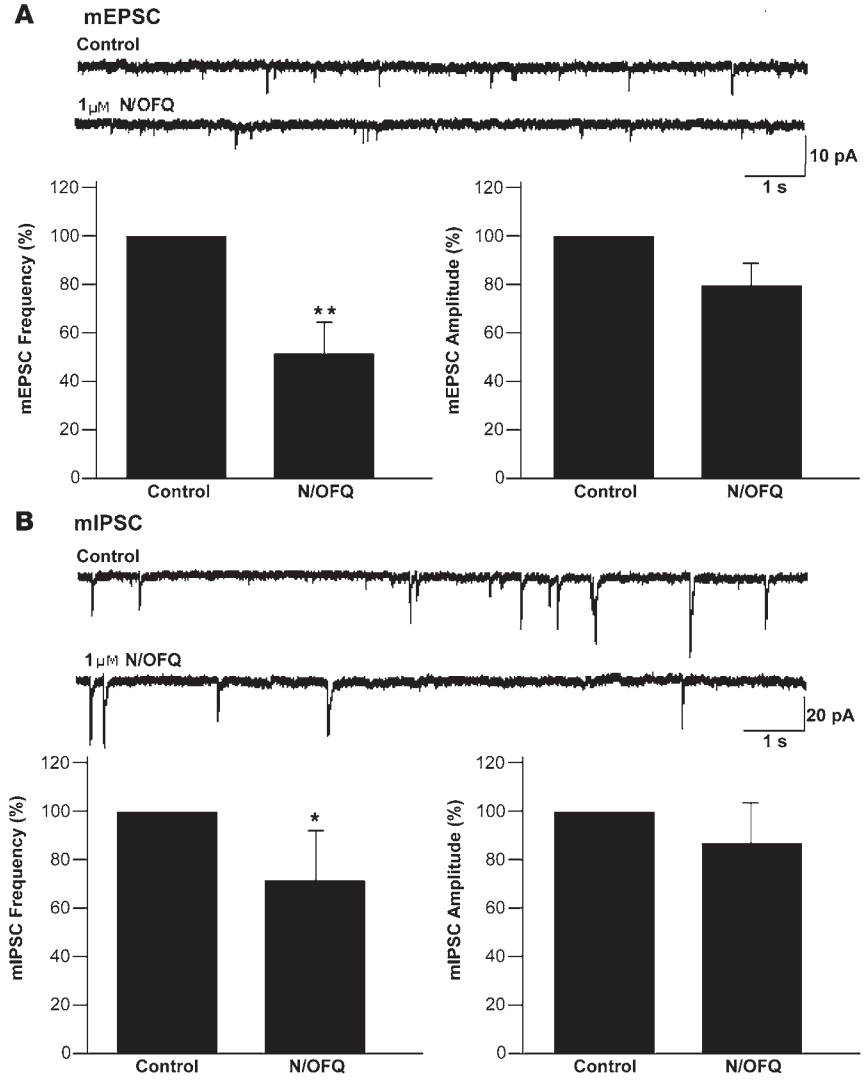

Figure 6
N/OFQ reduces the frequency of both mEPSCs and mIPSCs. (**A**) Representative traces showing mEPSCs in the presence and absence of N/OFQ (1 μM) and bar graphs summarizing the effects on mEPSC frequency and amplitude (mean ± SEM; $n = 8$). (**B**) Representative traces showing mIPSCs in the presence and absence of N/OFQ (1 μM) and bar graphs summarizing the effects on mIPSC frequency and amplitude (mean ± SEM; $n = 8$). $^{*}P < 0.05$, $^{**}P < 0.01$.

dendrites (Figure 1A). The origin(s) of the N/OFQ input to the Hcrt cells is unclear at this time and, given the number of potential N/OFQ sources (17), would be difficult to identify.

Since the original description, the Hcrt peptides have been known to be excitatory (1). Excitatory effects of Hcrt peptides have since been demonstrated in many brain regions by multiple laboratories. Hcrt modulation of synaptic transmission by both presynaptic and postsynaptic mechanisms suggests that Hcrt can have a potent neuromodulatory effect on a variety of physiological systems in the CNS. In contrast, N/OFQ has been shown to hyperpolarize postsynaptic neurons by activating K^+ conductance in a variety of types of neurons. In the dentate gyrus, N/OFQ activates different types of K^+ currents, including GIRK, M current, and large-conductance Ca^{2+}-activated K^+ currents (BK) (39), and inhibits L-, N-, and P/Q-type calcium channels (40, 41). In the present study, N/OFQ caused a long-lasting hyperpolarization and decreased input resistance; it also blocked the spontaneous firing of action potentials of Hcrt neurons (Figure 1, B and C). The I-V relationship of Hcrt neuronal responses in the presence and absence of N/OFQ is consistent with the actions of N/OFQ being mediated through activation of GIRK channels (Figure 3C). N/OFQ also inhibited high-voltage–activated Ca^{2+}currents (Figure 3D) and decreased cytoplasmic Ca^{2+} in Hcrt neurons in a concentration-dependent manner (Figure 3, E and F); both of these actions may contribute to inhibition of Hcrt neurons. N/OFQ (1 μM) decreased the frequency of both sEPSC/sIPSCs and mEPSC/mIPSCs with little effect on the amplitude of these events (Figures 4–6). These observations suggest that N/OFQ inhibition of Hcrt neurons is through both pre- and postsynaptic mechanisms.

Several lines of evidence suggest a role for the Hcrt system in nociceptive processing. Localization of Hcrt fibers to the hypothalamus, thalamus, and periaqueductal gray is consistent with a role in sensory processing (3, 4). Robust Hcrt projections exist from the hypothalamus to lamina I of the spinal cord (42), and Hcrt modulates nociceptive pathways (43). Behavioral studies show that Hcrt-1 is analgesic when given i.c.v. or i.v., but not s.c., in mouse and rat models of nociception and hyperalgesia (8–10). The efficacy of Hcrt-1 was similar to that of morphine in the hot-plate test and the carrageenan-induced thermal hyperalgesia test. Hcrt-1–induced analgesic effects were confirmed, and involvement of the opiate system was ruled out because Hcrt-1 analgesia was blocked by the Hcrt receptor (HcrtR) antagonist SB-334867 but

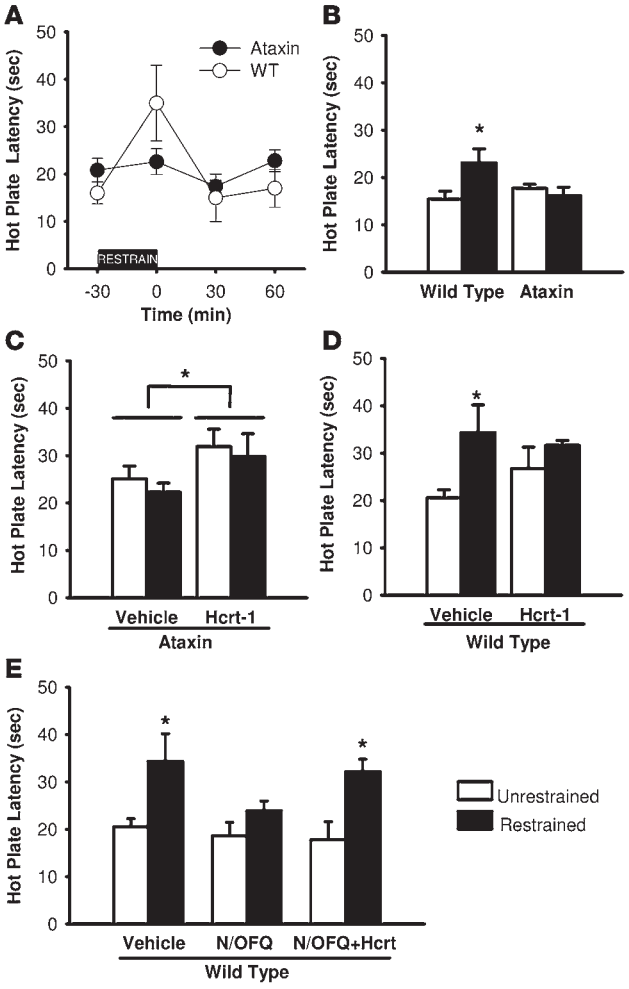

Figure 7
Inverse modulation of SIA by the Hcrt and N/OFQ systems. (**A**) SIA occurs in WT but not *orexin/ataxin* mice. From –30 to 0 minutes, mice (n = 8) were restrained; this was followed immediately by a hot-plate test at 0 minutes and again at 30 and 60 minutes following restraint. (**B**) SIA occurs in WT but not in *orexin/ataxin-3* mice. Post-hoc tests revealed a significant increase in hot-plate latency in WT mice after 30 minutes of restraint stress ($P < 0.05$) but not in *orexin/ataxin-3* mice. (**C**) Hcrt-1 administration produced acute analgesia. Hcrt-1 (1.5 nmol/mouse, i.c.v.) caused acute analgesia in both unrestrained and restrained animals compared with vehicle groups ($P \leq 0.05$), mimicking SIA in *orexin/ataxin-3* mice. (**D**) SIA occurs in WT mice subjected to i.c.v. injections. WT mice (n = 8 per group) were subjected to 30-minute restraint immediately after i.c.v. injection of either vehicle or Hcrt-1. (**E**) N/OFQ blocks SIA, and coapplication of Hcrt-1 with N/OFQ restores it in WT mice. WT mice (n = 8 per group) were subjected to 30-minute restraint immediately after i.c.v. injection of vehicle alone, vehicle plus N/OFQ, or a combination of the 2 neuropeptides. N/OFQ (1 nmol/mouse) inhibited SIA compared with vehicle restraint ($P = 0.044$) to a latency that was no different ($P = 0.503$) than in the unrestrained i.c.v. vehicle-injected WT mice shown in **D**. Coadministration of Hcrt-1 (1.5 nmol/mouse) with N/OFQ (1 nmol/mouse) restored SIA relative to vehicle/unrestrained mice ($P = 0.026$). Significance of differences compared with vehicle/unrestrained WT mice was determined by Fisher's protected least significant difference test. *$P < 0.05$ compared with respective controls. Error bars represent SEM.

not by naloxone (8–10). HcrtR antagonists had no effect in baseline acute nociceptive tests but, under inflammatory conditions, were prohyperalgesic, suggesting a tonic inhibitory Hcrt drive under these conditions (8). We demonstrated a deficit in SIA in *orexin/ataxin-3* mice, even though these transgenic mice display normal baseline thermal pain threshold and adequate analgesic response to exogenously applied Hcrt-1 (Figure 7, B and C), consistent with previous results determined in *prepro-orexin* null mice (12). Together, these results suggest that stressors such as immobilization, foot shock, and chemical-induced inflammatory pain can activate Hcrt neurons and pain inhibitory pathways (12).

Although the initial studies of N/OFQ suggested that it was pronociceptive, since i.c.v. N/OFQ resulted in a decrease in hot-plate escape jumping latency (13) and a decrease in tail-flick latency (14), it was later demonstrated that i.c.v. N/OFQ blocked stress-induced as well as opioid-mediated antinociception (44) and, like Hcrt, probably has no effect on baseline thermal pain threshold (45). The NOP receptor and N/OFQ precursor protein mRNA has been demonstrated in pain-processing pathways (17, 38), but the physiological actions of N/OFQ seem to be quite complicated. Many of its activities, including its antiopiate action, appear to be region and assay specific. Although antiopioid when injected i.c.v., N/OFQ can be analgesic in the spinal cord (46, 47) and an effective analgesic when injected intrathecally in chronic-pain models (48). The relative activities of N/OFQ agonists and antagonists in chronic-pain models are not clear since both N/OFQ and the potent and selective NOP antagonist SB-612111 have been reported to show antihyperalgesic activity (48, 49).

To explore the mechanism underlying the N/OFQ effect on SIA, we extended our in vitro studies to in vivo behavioral analysis. Since N/OFQ-containing fibers contact Hcrt cell bodies and NOP receptor activation leads to attenuation of Hcrt neuron activity, it follows that NOP receptor activation might lead to concomitant attenuation of Hcrt-mediated physiological actions. This suggestion is consistent with known examples of differential modulation of behavior and cellular physiology by these 2 systems, including their respective induction and attenuation of SIA. Excitatory signals mediated by the Hcrt system not only play a crucial role in the stability of arousal and alertness but also contribute to the stress response (11) and therefore, potentially, to SIA (50). The Hcrt system is thus implicated in anxiogenesis which, under pathological conditions, leads to addiction (35–37). In contrast, N/OFQ consistently produces inhibitory effects on neuronal activity, attenuates stress responses, and depresses SIA (16, 40, 41). In the present study, not only did we confirm the necessity of a functional Hcrt system for the generation of SIA (Figure 7B) and the attenuation of SIA by i.c.v. administration of N/OFQ but, more importantly, this suppression of SIA was restored by simultaneous i.c.v. administration of Hcrt-1 (Figure 7E). Since Hcrt does not directly antagonize N/OFQ, these results suggest that exogenous Hcrt triggers downstream neurotransmitter systems (such as serotonin, histamine, and possibly the opioid system) that participate in the generation of SIA (16). In *orexin/ataxin-3* mice in which the Hcrt neurons have degenerated, little if any Hcrt exists to trigger downstream systems to thereby generate SIA. Conversely, exogenously applied Hcrt-1 is able to activate pain inhibitory pathways, manifested by an increase in hot-plate latency in *orexin/ataxin-3* mice, whether the animals were stressed or not (Figure 7C). Considering the anatomical, electrophysiological, and behavioral data, these results suggest

that N/OFQ acts by depressing endogenous Hcrt release to block SIA rather than by inhibiting the downstream analgesic effect of stress. Due to N/OFQ's multiple sites of action, it is possible that i.c.v. administration of N/OFQ leads to inhibition of additional neuronal pathways that also manifest in an attenuation of SIA. Additional studies with local injections of N/OFQ into the PLH will clarify the precise effects of N/OFQ on the Hcrt system with respect to SIA and other actions.

In conclusion, the results from a combination of anatomical, cellular electrophysiological, and behavioral studies establish a previously unrecognized interaction between the Hcrt and N/OFQ systems. Behavioral studies conducted in both WT and *orexin/ataxin*-3 mice indicate that the Hcrt system is involved in the development of SIA and that interaction between N/OFQ and Hcrt systems can provide "fine tuning" of this adaptive behavior. Because the Hcrt neurons are so highly localized and since virtually every Hcrt cell was potently inhibited by N/OFQ, these studies also suggest that N/OFQ and potentially small molecule agonists of NOP receptors are likely to modulate a variety of Hcrt-mediated actions including sleep/wake, stress, reward, and addiction. The interaction between these systems may also be relevant to dysfunctional conditions resulting from excessive stress such as anxiety and posttraumatic stress disorder.

Methods

Experimental animals. Mouse studies were approved by the SRI International Institutional Animal Care and Use Committee and performed in conformance with the US Public Health Service Guidelines on Care and Use of Animals in Research. The *orexin/EGFP* and *orexin/ataxin*-3 mice were from breeding colonies at SRI International; the *orexin/YC2.1* mice were maintained at the University of Tsukuba. Mice of both sexes were used for in vitro studies; only male mice were used for behavioral studies. Transgenic mice were backcrossed onto a C57BL/6 background for at least 10 generations and maintained on this isogenic background. Mice were group housed with free access to food and water under a 12-hour light/12-hour dark cycle for at least 2 weeks before use in an experiment.

Perfusion/fixation. Mice were euthanized with Beuthanasia-D (0.5–1 ml/kg, i.p.; 390 mg/ml pentobarbitone, 50 mg/ml phenytoin; Schering-Plough), followed by transcardial perfusion of 10 ml 0.9% saline and then 30 ml 4% paraformaldehyde in 0.1 M phosphate buffer (PB). Brains were removed, equilibrated in ascending sucrose solutions (10%, 20%, and 30% in PB), sectioned at 40 μm on a freezing microtome for light microscopy or 10 μm on a cryostat for confocal microscopy, and the sections collected in PB containing 0.1% sodium azide.

Immunohistochemistry. Brain sections (10 μm) were treated with 0.3% H_2O_2 to quench endogenous peroxidases and then incubated overnight in primary anti-N/OFQ (1:5,000; RA10106, anti-FGGFTGARKSARKLANQ, Neuromics) and anti-orexin-B (1:5,000; sc-8071, Santa Cruz Biotechnology Inc.) antisera at 4°C with agitation. Sections were incubated in blocking buffer for 1 hour, followed by a 2-hour incubation at room temperature in secondary antisera (Alexa Fluor 546 donkey anti-goat [1:750] and 488 donkey anti-rabbit [1:500]; Molecular Probes, Invitrogen). As a negative control, additional sections were treated similarly, but the primary antibody was omitted. Preadsorption with the N/OFQ peptide FGGFTGARKSARKLANQ was used as a positive control and blocked all specific staining as also found by others (51). Although the exact peptide sequence used as an immunogen to produce the orexin-B antiserum has not been disclosed by the manufacturer, this antiserum has also been characterized previously (52). Following immunohistochemistry procedures, sections were mounted onto slides (Superfrost Plus; Fisher Scientific), air-dried, dehydrated in ethanol, cleared in xylenes, and coverslipped. Brain sections were examined under light microscopy (DM5000B; Leica) equipped for fluorescence and a confocal microscope (Nikon ×60 PlanApo [1.40 oil] objective, 3.0 iris setting on a Bio-Rad MRC 1024).

EM. Brain sections first were immunostained for N/OFQ with rabbit polyclonal antiserum against N/OFQ (1:1,000; Neuromics), incubated in donkey anti-rabbit IgG, avidin-biotin complex (ABC) (VECTASTAIN ABC Systems; Vector Laboratories), and then visualized with a modified version of the nickel-diaminobenzidine (Ni-DAB) reaction as described (11). The sections were further incubated in goat anti-Hcrt antiserum (1:1,000; Phoenix Pharmaceuticals Inc.) for 24 hours at 4°C, followed by secondary antibody (donkey anti-goat IgG diluted 1:50 in PB) and goat peroxidase-antiperoxidase (PAP) (1:100 in PB). The tissue-bound peroxidase was visualized by a light brown DAB reaction. After immunostaining, the sections were thoroughly rinsed in PB and processed for correlated EM. Color photographs and images were taken of Hcrt-immunoreactive cells contacted by putative N/OFQ-immunoreactive axon terminals. Blocks were trimmed using the color picture of previously identified cells and boutons as a guide. Ribbons of serial ultrathin sections were collected on Formvar-coated single slot grids and examined under EM as previously described (11).

Hypothalamic slice preparation. *Orexin/EGFP* mice (2–5 weeks old) and *orexin/YC2.1* mice (3–8 weeks of age) from both sexes were used. Hypothalamic slice preparation and recording conditions followed the procedures described previously (20).

Electrophysiologic recordings. The procedures used for patch clamp recording of Hcrt neurons, including isolation of sEPSCs, sIPSCs, mEPSCs, and mIPSCs, have been described previously (20). The frequency of sEPSCs or sIPSCs was measured using pCLAMP (v. 9.2; Molecular Devices); only those events with amplitudes greater than 10 pA were used. Frequency and amplitudes were calculated as a mean of an 180-second recording period.

Ca^{2+} imaging of Hcrt neurons. Optical recordings of hypothalamic slices taken from *orexin/YC2.1* mice were performed on a fluorescence microscope (BX51WI; Olympus) equipped with a cooled CCD camera (Cascade 650; Roper Scientific) controlled by MetaFluor 5.0.7 software (Universal Imaging), as described previously (24).

TaqMan PCR analyses. Hcrt mRNA levels in *orexin/ataxin-3* and WT mice were quantified using real-time fluorescence detection as described previously (53).

Video assessment of immobility in orexin/ataxin-3 mice. Mice were individually housed for at least 1 week prior to video recording. Immediately prior to lights off on the day of observation, mice were taken from the colony room to an adjacent room in which one infrared camera was positioned directly above the cage and another positioned to the side of the cage. Food and water were provided in dishes on the cage floor throughout the recording. Video data were collected beginning at the onset of darkness and were scored by a trained observer who was blind to treatment and genotype. The observer documented the times of onset and offset of any "sleep" episodes (episodes ≥5 seconds when the mouse was in a prone position in its nesting area and did not exhibit any detectable purposeful movements) or "cataplexy" (an immediate transition from an active waking state characterized by locomotion, eating, or rearing to a complete loss of muscle tone lasting at least 5 seconds). Since an unequivocal definition of cataplexy would require simultaneous measurement of EEG and electromyogram (which was not done in the present study), we conservatively report here immobility time and the frequency of cataplexy-like events during the first 2 hours of the dark phase for mice of both genotypes.

i.c.v. injections. Animals that received i.c.v. injections were lightly anesthetized with isoflurane and received a unilateral injection (2.0 mm caudal and 2.0 mm lateral with respect to bregma and –2.5 mm ventral

from the skull surface). Drugs were injected in a volume of 2 μl. Thirty minutes after i.c.v. injections, animals fully recovered from anesthesia were tested for hot-plate and/or tail-flick latencies, either with or without restraint stress.

Hot-plate test. All behavioral assessments were conducted between Zeitgeber time 2 (ZT2) and ZT12 (ZT0 = light on) under normal room lighting by an experimenter blind to genotype or experimental treatment. *Orexin/ataxin-3* mice and control WT mice used in these studies did not differ in body weight. Control animals were either littermates or age-matched mice derived from the same breeding colony that had been derived by backcrossing transgenics into the B6 strain over more than 10 generations. Animals were placed on a 52°C hot plate (Hot-Plate Analgesia Meter; Columbus Instruments) and the latency to hind-paw licking or fanning was recorded. For SIA evaluation, to avoid any potential stress induced by repetitive thermal pain measures, only 1 measurement was made at a given time point for each subject. A 60-second cut-off latency was used to avoid tissue damage.

Tail-flick test. Tail-flick assays were performed immediately after hot-plate assays. Acute nociception was assessed using an analgesia instrument (Stoelting) that uses radiant heat. During testing, a focused beam of light was applied to the lower half of the animal's tail, and light intensity was set to provide a baseline tail-flick latency of approximately 4 seconds in WT mice. A 15-second cutoff was used to prevent tissue damage.

Statistics. All data are presented as mean ± SEM. For behavioral studies, we tested for group differences using a 2-way ANOVA, with one factor being genotype and the other being a 3-category treatment group variable (control, drug, or behavioral manipulation, e.g., restraint). If the ANOVA was statistically significant, Fisher's PLSD was used to determine group differences. The level of significance was set at $P < 0.05$ for all tests.

Acknowledgments

This work was supported by NIH grants R43MH072162, RO1MH61755, RO1AG020584, R01DA020811, R01DK070039, R01DK060711, R44RR017182, and R21NS057052. J. Hara was a fellow of the Uehara Memorial Foundation. We are grateful to N. Zaveri (SRI International) for providing the NOP antagonist SR14148.

Received for publication January 23, 2008, and accepted in revised form May 7, 2008.

Address correspondence to: Xinmin (Simon) Xie, AfaSci Inc., 2633 Martinez Drive, Burlingame, California 94010, USA. Phone: (650) 692-6051; Fax: (650) 692-6051; E-mail: simonxie@afasci.com. Or to: Thomas S. Kilduff, Biosciences Division, SRI International, Menlo Park, California 94025, USA. Phone: (650) 859-5509; Fax: (650) 859-3153; E-mail: thomas.kilduff@sri.com.

Takeshi Sakurai's present address is: Kanazawa University, Molecular Neuroscience and Integrative Physiology, Kanazawa, Ishikawa, Japan.

1. de Lecea, L., et al. 1998. The hypocretins: hypothalamus-specific peptides with neuroexcitatory activity. *Proc. Natl. Acad. Sci. U. S. A.* **95**:322–327.
2. Sakurai, T., et al. 1998. Orexins and orexin receptors: a family of hypothalamic neuropeptides and G protein-coupled receptors that regulate feeding behavior. *Cell.* **92**:573–585.
3. Nambu, T., et al. 1999. Distribution of orexin neurons in the adult rat brain. *Brain Res.* **827**:243–260.
4. Peyron, C., et al. 1998. Neurons containing hypocretin (orexin) project to multiple neuronal systems. *J. Neurosci.* **18**:9996–10015.
5. Kilduff, T.S. 2005. Hypocretin/orexin: maintenance of wakefulness and a multiplicity of other roles. *Sleep Med. Rev.* **9**:227–230.
6. de Lecea, L., et al. 2006. Addiction and arousal: alternative roles of hypothalamic peptides. *J. Neurosci.* **26**:10372–10375.
7. Sakurai, T. 2007. The neural circuit of orexin (hypocretin): maintaining sleep and wakefulness. *Nat. Rev. Neurosci.* **8**:171–181.
8. Bingham, S., et al. 2001. Orexin-A, an hypothalamic peptide with analgesic properties. *Pain.* **92**:81–90.
9. Kajiyama, S., et al. 2005. Spinal orexin-1 receptors mediate anti-hyperalgesic effects of intrathecally-administered orexins in diabetic neuropathic pain model rats. *Brain Res.* **1044**:76–86.
10. Mobarakeh, J.I., et al. 2005. Enhanced antinociception by intracerebroventricularly and intrathecally-administered orexin A and B (hypocretin-1 and -2) in mice. *Peptides.* **26**:767–777.
11. Winsky-Sommerer, R., et al. 2004. Interaction between the corticotropin-releasing factor system and hypocretins (orexins): a novel circuit mediating the stress response. *J. Neurosci.* **24**:11439–11448.
12. Watanabe, S., Kuwaki, T., Yanagisawa, M., Fukuda, Y., and Shimoyama, M. 2005. Persistent pain and stress activate pain-inhibitory orexin pathways. *Neuroreport.* **16**:5–8.
13. Meunier, J.C., et al. 1995. Isolation and structure of the endogenous agonist of opioid receptor- like ORL1 receptor. *Nature.* **377**:532–535.
14. Reinscheid, R.K., et al. 1995. Orphanin FQ: a neuropeptide that activates an opioidlike G protein-coupled receptor. *Science.* **270**:792–794.
15. Koster, A., et al. 1999. Targeted disruption of the orphanin FQ/nociceptin gene increases stress susceptibility and impairs stress adaptation in mice. *Proc. Natl. Acad. Sci. U. S. A.* **96**:10444–10449.
16. Rizzi, A., et al. 2001. Endogenous nociceptin signaling and stress-induced analgesia. *Neuroreport.* **12**:3009–3013.
17. Neal, C.R., Jr., et al. 1999. Localization of orphanin FQ (nociceptin) peptide and messenger RNA in the central nervous system of the rat. *J. Comp. Neurol.* **406**:503–547.
18. Amit, Z., and Galina, Z.H. 1986. Stress-induced analgesia: adaptive pain suppression. *Physiol. Rev.* **66**:1091–1120.
19. Amit, Z., and Galina, Z.H. 1988. Stress induced analgesia plays an adaptive role in the organization of behavioral responding. *Brain Res. Bull.* **21**:955–958.
20. Xie, X., et al. 2006. GABA(B) receptor-mediated modulation of hypocretin/orexin neurones in mouse hypothalamus. *J. Physiol.* **574**:399–414.
21. Yamanaka, A., et al. 2003. Hypothalamic orexin neurons regulate arousal according to energy balance in mice. *Neuron.* **38**:701–713.
22. Yamanaka, A., Muraki, Y., Tsujino, N., Goto, K., and Sakurai, T. 2003. Regulation of orexin neurons by the monoaminergic and cholinergic systems. *Biochem. Biophys. Res. Commun.* **303**:120–129.
23. Li, Y., Gao, X.B., Sakurai, T., and van den Pol, A.N. 2002. Hypocretin/Orexin excites hypocretin neurons via a local glutamate neuron-A potential mechanism for orchestrating the hypothalamic arousal system. *Neuron.* **36**:1169–1181.
24. Tsujino, N., et al. 2005. Cholecystokinin activates orexin/hypocretin neurons through the cholecystokinin A receptor. *J. Neurosci.* **25**:7459–7469.
25. Hara, J., et al. 2001. Genetic ablation of orexin neurons in mice results in narcolepsy, hypophagia, and obesity. *Neuron.* **30**:345–354.
26. Zaveri, N.T., et al. 2004. A novel series of piperidin-4-yl-1,3-dihydroindol-2-ones as agonist and antagonist ligands at the nociceptin receptor. *J. Med. Chem.* **47**:2973–2976.
27. Hoang, Q.V., Bajic, D., Yanagisawa, M., Nakajima, S., and Nakajima, Y. 2003. Effects of orexin (hypocretin) on GIRK channels. *J. Neurophysiol.* **90**:693–702.
28. Pitcher, G.M., Yashpal, K., Coderre, T.J., and Henry, J.L. 1995. Mechanisms underlying antinociception provoked by heterosegmental noxious stimulation in the rat tail-flick test. *Neuroscience.* **65**:273–281.
29. Thannickal, T., et al. 2000. Reduced number of hypocretin neurons in human narcolepsy. *Neuron.* **27**:469–474.
30. Peyron, C., et al. 2000. A mutation in a case of early onset narcolepsy and a generalized absence of hypocretin peptides in human narcoleptic brains. *Nat. Med.* **6**:991–997.
31. Chemelli, R.M., et al. 1999. Narcolepsy in orexin knockout mice: molecular genetics of sleep regulation. *Cell.* **98**:437–451.
32. Gerashchenko, D., et al. 2001. Hypocretin-saporin induced lesion of the lateral hypothalamus produces narcoleptic-like sleep behavior in the rat. *J. Neurosci.* **21**:7273–7283.
33. Lin, L., et al. 1999. The sleep disorder canine narcolepsy is caused by a mutation in the hypocretin (orexin) receptor 2 gene. *Cell.* **98**:365–376.
34. Samson, W.K., Taylor, M.M., and Ferguson, A.V. 2005. Non-sleep effects of hypocretin/orexin. *Sleep Med. Rev.* **9**:243–252.
35. Boutrel, B., et al. 2005. Role for hypocretin in mediating stress-induced reinstatement of cocaine-seeking behavior. *Proc. Natl. Acad. Sci. U. S. A.* **102**:19168–19173.
36. Harris, G.C., Wimmer, M., and Aston-Jones, G. 2005. A role for lateral hypothalamic orexin neurons in reward seeking. *Nature.* **437**:556–559.
37. Narita, M., et al. 2006. Direct involvement of orexinergic systems in the activation of the mesolimbic dopamine pathway and related behaviors induced by morphine. *J. Neurosci.* **26**:398–405.
38. Neal, C.R., Jr., et al. 1999. Opioid receptor-like (ORL1) receptor distribution in the rat central nervous system: comparison of ORL1 receptor mRNA expression with (125)I-[(14)Tyr]-orphanin FQ binding. *J. Comp. Neurol.* **412**:563–605.
39. Shirasaki, T., Houtani, T., Sugimoto, T., and Matsuda, H. 2001. Spontaneous transient outward currents: modulation by nociceptin in murine dentate gyrus granule cells. *Brain Res.* **917**:191–205.

40. Connor, M., Vaughan, C.W., Chieng, B., and Christie, M.J. 1996. Nociceptin receptor coupling to a potassium conductance in rat locus coeruleus neurones in vitro. *Br. J. Pharmacol.* **119**:1614–1618.
41. Knoflach, F., Reinscheid, R.K., Civelli, O., and Kemp, J.A. 1996. Modulation of voltage-gated calcium channels by orphanin FQ in freshly dissociated hippocampal neurons. *J. Neurosci.* **16**:6657–6664.
42. van den Pol, A.N. 1999. Hypothalamic hypocretin (orexin): robust innervation of the spinal cord. *J. Neurosci.* **19**:3171–3182.
43. Grudt, T.J., van den Pol, A.N., and Perl, E.R. 2002. Hypocretin-2 (orexin-B) modulation of superficial dorsal horn activity in rat. *J. Physiol.* **538**:517–525.
44. Mogil, J.S., et al. 1996. Orphanin FQ is a functional anti-opioid peptide. *Neuroscience.* **75**:333–337.
45. Vanderah, T.W., et al. 1998. Orphanin-FQ/nociceptin: lack of anti nociceptive, hyperalgesic or allodynic effects in acute thermal or mechanical tests following intracerebroventricular or intrathecal administration to mice or rats. *Eur. J. Pain.* **2**:267–278.
46. Tian, J.H., et al. 1997. Bidirectional modulatory effect of orphanin FQ on morphine-induced analgesia: antagonism in brain and potentiation in spinal cord of the rat. *Br. J. Pharmacol.* **120**:676–680.
47. Xu, X.J., Hao, J.X., and Wiesenfeld-Hallin, Z. 1996. Nociceptin or antinociceptin: potent spinal antinociceptive effect of orphanin FQ/nociceptin in the rat. *Neuroreport.* **7**:2092–2094.
48. Courteix, C., et al. 2004. Evidence for an exclusive antinociceptive effect of nociceptin/orphanin FQ, an endogenous ligand for the ORL1 receptor, in two animal models of neuropathic pain. *Pain.* **110**:236–245.
49. Zaratin, P.F., et al. 2004. Modification of nociception and morphine tolerance by the selective opiate receptor-like orphan receptor antagonist (–)-cis-1-methyl-7-[[4-(2,6-dichlorophenyl)piperidin-1-yl]methyl]-6,7,8,9- tetrahydro-5H-benzocyclohepten-5-ol (SB-612111). *J. Pharmacol. Exp. Ther.* **308**:454–461.
50. Sakamoto, F., Yamada, S., and Ueta, Y. 2004. Centrally administered orexin-A activates corticotropin-releasing factor-containing neurons in the hypothalamic paraventricular nucleus and central amygdaloid nucleus of rats: possible involvement of central orexins on stress-activated central CRF neurons. *Regul. Pept.* **118**:183–191.
51. Foradori, C.D., et al. 2007. Orphanin FQ: evidence for a role in the control of the reproductive neuroendocrine system. *Endocrinology.* **148**:4993–5001.
52. Deurveilher, S., Lo, H., Murphy, J.A., Burns, J., and Semba, K. 2006. Differential c-Fos immunoreactivity in arousal-promoting cell groups following systemic administration of caffeine in rats. *J. Comp. Neurol.* **498**:667–689.
53. Terao, A., et al. 2000. Prepro-hypocretin (prepro-orexin) expression is unaffected by short-term sleep deprivation in rats and mice. *Sleep.* **23**:867–874.